Journal of Power Sources xxx (2016) 1–5

Contents lists available at ScienceDirect

Journal of Power Sources

journal homepage: www.elsevier.com/locate/jpowsour

Capacitance of $Ti_3C_2T_x$ MXene in ionic liquid electrolyte

Zifeng Lin [a, b], Daffos Barbara [a, b], Pierre-Louis Taberna [a, b], Katherine L. Van Aken [c], Babak Anasori [c], Yury Gogotsi [c], Patrice Simon [a, b, *]

[a] CIRIMAT, Université de Toulouse, CNRS, INPT, UPS, 118, route de Narbonne, 31062 Toulouse cedex 9, France
[b] Reseau sur le Stockage Electrochimique de l'Energie (RS2E), FR CNRS 3459, France
[c] Department of Materials Science & Engineering, A.J. Drexel Nanomaterials Institute, Drexel University, Philadelphia, PA 19104, USA

HIGHLIGHTS

- $Ti_3C_2T_x$-ionogel film was prepared by vacuum filtration and ionic liquid immersion.
- Capacitance of 70 F g^{-1} in a voltage window of 3 V was achieved in EMI-TFSI.
- High power performance was obtained as shown by the rectangular CVs shape.

ARTICLE INFO

Article history:
Received 9 February 2016
Received in revised form
5 April 2016
Accepted 7 April 2016
Available online xxx

Keywords:
Supercapacitors
MXene
$Ti_3C_2T_x$
Ionogel
Ionic liquid

ABSTRACT

$Ti_3C_2T_x$ MXene, a two-dimensional (2D) early transition metal carbide, has shown an extremely high volumetric capacitance in aqueous electrolytes, but in a narrow voltage window (less than 1.23 V). The utilization of MXene materials in ionic liquid electrolytes with a large voltage window has never been addressed. Here, we report the preparation of the $Ti_3C_2T_x$ MXene ionogel film by vacuum filtration for use as supercapacitor electrodes operating in 1-Ethyl-3-methylimidazolium bis(trifluoromethylsulfonyl) imide (EMI-TFSI) neat ionic liquid electrolyte. Due to the disordered structure of the $Ti_3C_2T_x$ hydrogel film and a stable spacing after vacuum drying, achieved through ionic liquid electrolyte immersion of the $Ti_3C_2T_x$ hydrogel film, the $Ti_3C_2T_x$ surface became accessible to EMI^+ and $TFSI^-$ ions. A capacitance of 70 F g^{-1} together with a large voltage window of 3 V was obtained at a scan rate of 20 mV s^{-1} in neat EMI-TFSI electrolyte. The electrochemical signature indicates a capacitive behavior even at a high scan rate (500 mV s^{-1}) and a high power performance. This work opens up the possibilities of using MXene materials with various ionic liquid electrolytes.

1. Introduction

MXenes are a novel family of two-dimensional (2D) early transition metal carbides and carbonitrides which are produced by selective etching of the A element from MAX phases. MXenes are usually referred to as $M_{n+1}X_nT_x$, where M is an early transition metal, X is carbon and/or nitrogen, T represents surface terminations (=O, −OH, and/or −F), n = 1, 2, or 3, and x is the number of terminating groups per formula unit [1–4]. MXenes have shown great potential as electrode materials for both Li-ion batteries [5–10] and supercapacitors [1,11–13] where high volumetric capacitance up to 900 F cm^{-3} was reported in aqueous electrolyte for the latter [1]. However, when a colloidal solution of MXene flakes is filtered for MXene paper electrode preparation, they restack and once the film was completely dried, the *c*-lattice parameter dropped dramatically. In other words, their interlayer spacing becomes smaller and this process was irreversible [14]. MXene flakes' restacking during filtration and their small interlayer spacing limit the accessibility to electrolyte ions, especially the large ions of ionic liquids, hindering the full utilization of the surface area thus leading to poor electrochemical behavior [15]. Improvement has been made by adding carbon nanotubes or graphene materials to MXene [15,16] and making composite materials, which also enhanced the capacitance of MXene-based supercapacitors in organic electrolytes [17]. However, the use of pure MXenes in ionic liquid electrolytes has not been reported yet. Ionic liquids (ILs) are solvent-free salts that are liquid at room temperature. They are promising for energy storage devices due to their

* Corresponding author. CIRIMAT, Université de Toulouse, CNRS, INPT, UPS, 118, route de Narbonne, 31062 Toulouse cedex 9, France.
E-mail address: simon@chimie.ups-tlse.fr (P. Simon).

http://dx.doi.org/10.1016/j.jpowsour.2016.04.035
0378-7753/

low vapor pressure, electrochemical stability, and nonflammability. They can also operate at very high voltages compared to other electrolytes for energy storage devices (>4 V in some cases) [18]. Nevertheless, one drawback is the low ion mobility and high viscosity, making such electrolytes less suitable for highly porous electrode materials or layered materials with a small interlayer distance.

In this paper, we propose a facile route for making a $Ti_3C_2T_x$ hydrogel film by vacuum filtration, to prevent restacking of the flakes. The prepared $Ti_3C_2T_x$ hydrogel film was further immersed in the ionic liquid electrolyte; after vacuum drying, ionic liquid (low vapor pressure and thermally stable) remained in the $Ti_3C_2T_x$ film, which increased the MXene interflake spacing and prevented restacking. Hence, the surface of $Ti_3C_2T_x$ flakes became accessible to the large size cations and anions of the ionic liquid electrolyte. Using this $Ti_3C_2T_x$ ionogel film as electrode material for supercapacitors in EMI-TFSI electrolyte, a capacitance of 70 F g^{-1} within a large voltage window of 3 V is reported, as well as a high power performance.

2. Experimental

2.1. Material preparation

Multilayer $Ti_3C_2T_x$ particles were prepared by selective etching of Al from Ti_3AlC_2 by a mixture solution of hydrochloric acid (HCl) and lithium fluoride (LiF) [1]. Briefly, 2 g LiF was added to 40 mL 9 M HCl solution, followed by the slow addition of 2 g of Ti_3AlC_2. After etching for 24 h at 35 °C, the obtained $Ti_3C_2T_x$ flakes were washed until a pH value of ~6 was achieved. The delaminated $Ti_3C_2T_x$ colloidal solution was prepared by 1-h sonication, followed by 1-h centrifugation at 3500 rpm to eliminate the sediment.

2.2. Film preparation

$Ti_3C_2T_x$ dried film and hydrogel film were both prepared by vacuum filtration of delaminated $Ti_3C_2T_x$ colloidal solution as shown in Fig. 1. The dried film was prepared by vacuum filtration to completely expel water from inside. To make the hydrogel film (Fig. 1), the vacuum was disconnected immediately once there were no free $Ti_3C_2T_x$ colloidal flakes on the wet filtrate cake. After vacuum filtration, both films were immersed in acetone and carefully peeled off from the filter membrane. Compared to dried $Ti_3C_2T_x$ film, the hydrogel $Ti_3C_2T_x$ film is assumed to contain huge amounts of water and acetone between $Ti_3C_2T_x$ flakes. Afterward, the $Ti_3C_2T_x$ dried film was transferred to a vacuum oven for drying at 80 °C for 48 h and we henceforth will refer to it as dried film. The hydrogel film was immersed in EMI-TFSI electrolyte to exchange with water and acetone for more than 72 h, followed by 48 h of vacuum drying at 80 °C to remove the residual water and acetone and will henceforth be referred to as ionogel film.

2.3. Electrochemical tests

$Ti_3C_2T_x$ disc films were punched (with a diameter of 10 mm) after vacuum drying from both samples and used as electrodes directly without any binders. 1-ethyl-3-methylimidazolium bis-(trifluoromethylsulfonyl)-imide (EMI-TFSI) neat ionic liquid was used as the electrolyte. Two layers of separator (Celgard® 3501) were used together with platinum discs as current collectors. Two-electrode Swagelok symmetric cells were assembled and tested at room temperature by using a VMP3 potentiostat (Biologic, USA.). All supercapacitors were assembled in a glove box under argon atmosphere with water and oxygen contents less than 1 ppm.

Electrochemical impedance spectroscopy (EIS) measurements were carried out at open circuit voltage (OCV) with an amplitude of 10 mV at the frequency range from 200 kHz to 0.01 Hz. Capacitances were calculated from cyclic voltammograms (CVs) by measuring the slope of the integrated discharge charge Q versus cell voltage (V) plot. Since all the tests were performed using a symmetric cell, the gravimetric electrode capacitance was calculated using Equation (1):

$$C = \frac{2\Delta Q}{\Delta V \cdot m} \tag{1}$$

where C is the specific capacitance (F g^{-1}); $\Delta Q/\Delta V$ is the slope of the integrated discharge charge Q versus cell voltage plot; m is the mass of $Ti_3C_2T_x$ of one electrode (g). 3-electrode experiments (not shown) have confirmed that both positive and negative electrode exhibit similar gravimetric capacitance.

2.4. Characterization

X-ray diffraction (XRD) patterns of $Ti_3C_2T_x$ films were recorded

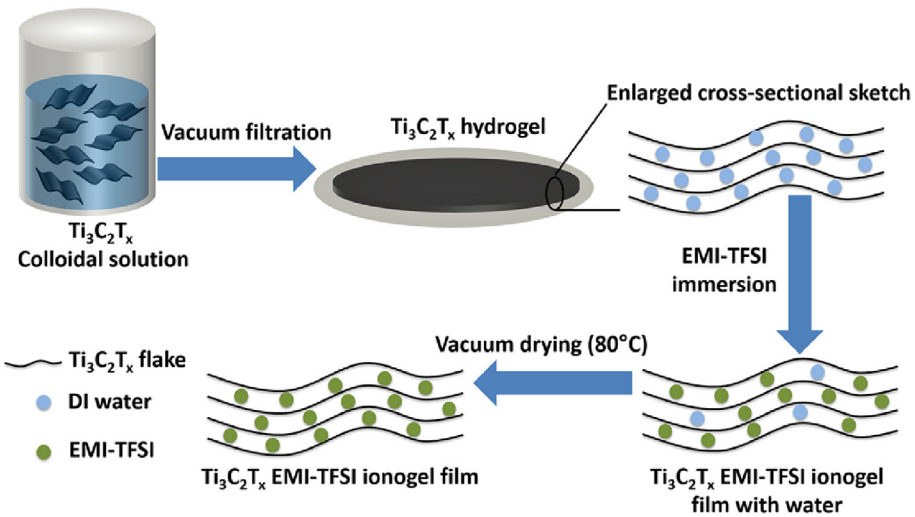

Fig. 1. Schematic of producing $Ti_3C_2T_x$ EMI-TFSI ionogel film.

Please cite this article in press as: Z. Lin, et al., Journal of Power Sources (2016), http://dx.doi.org/10.1016/j.jpowsour.2016.04.035

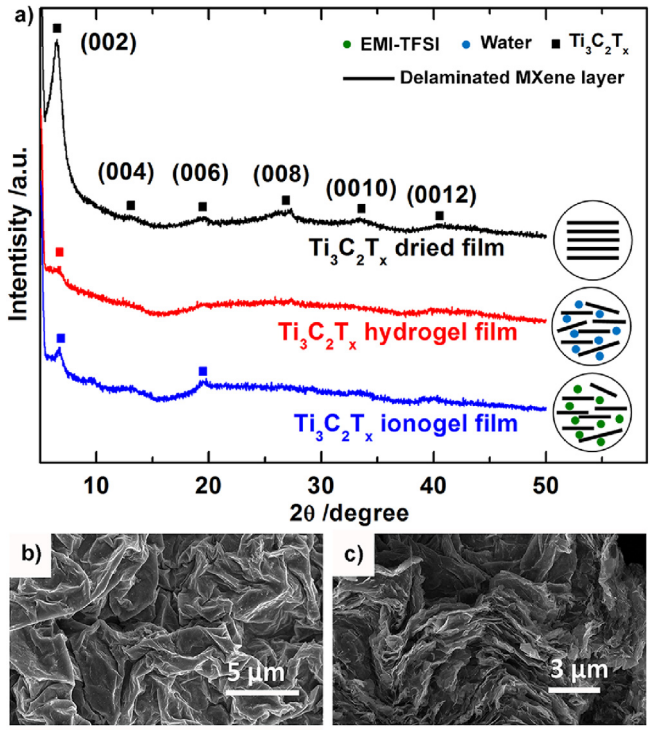

Fig. 2. a) XRD patterns of $Ti_3C_2T_x$ dried film, hydrogel film and ionogel film; b, c) SEM images of $Ti_3C_2T_x$ inogel film: b) top view; c) cross-sectional view.

by a Bruker D4 (Bruker, Germany) diffractometer using a Cu Kα radiation (λ = 0.154 nm) in the range 2θ = 5–50° at a step rate of 0.06° s^{-1}.

Scanning electron microscope (SEM) observations of the $Ti_3C_2T_x$ films were made using a FEG-SEM (EOL JSM 6700F, Japan).

3. Results and discussion

Fig. 2a presents the XRD diffraction patterns of the $Ti_3C_2T_x$ dried, hydrogel and ionogel films. For comparison, all tested films were cut with the same size and the same weight of MXene material. The (002) peak around 6.5° (corresponding to a *c*-lattice parameter of ~27 Å) in the dried film's XRD pattern evidences the existence of water between $Ti_3C_2T_x$ flakes [1]. It has been shown previously that vacuum drying at above 100 °C is needed to remove the water between MXene flakes [19]. The high intensity of the (002) peak and the presence of all (*00l*) peaks in the dried film can be ascribed to restacking of $Ti_3C_2T_x$ flakes. However, (*00l*) peak intensities, especially (002), decrease in the hydrogel and ionogel XRD patterns, which is due to the interruption of $Ti_3C_2T_x$ flakes restacking [20]. The nonperiodic (disordered) structure of the ionogel film vs. the dried film is believed to enhance the accessibility of cations and anions of ionic liquid electrolyte into the MXene layers.

SEM observations of the $Ti_3C_2T_x$ ionogel film are shown in Fig. 2b and c. The top view, Fig. 2b, presents many wrinkles on the $Ti_3C_2T_x$ flakes, which reveals a more disordered structure compared to the flat dried MXene paper shown in the previous studies [2,21]. From the cross-sectional view of the film in Fig. 2c, a less compact layered structure can be observed. The observed disordered structure is well consistent with the XRD results.

For comparison, the electrochemical performance of the dried $Ti_3C_2T_x$ film was first explored. The Nyquist plot (Fig. 3a) reveals a low contact resistance at high frequencies due to the compact structure of the film, but the resistance drastically increases when

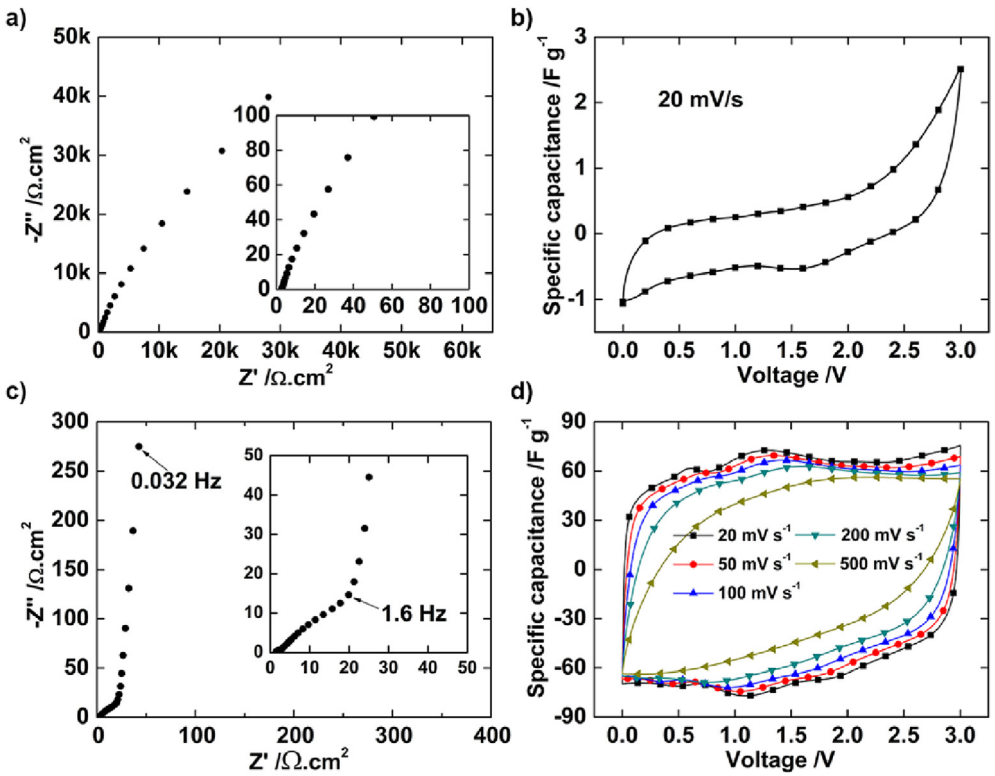

Fig. 3. a) Nyquist plot and b) CV of $Ti_3C_2T_x$ dried film tested in EMI-TFSI ionic liquid electrolyte. Electrochemical characterizations of $Ti_3C_2T_x$ ionogel film with mass loading of 0.76 mg cm^{-2} (mass of $Ti_3C_2T_x$ only): c) Nyquist plot of a 2-electrode Swagelok cell; d), CVs of a 2-electrode Swagelok cell at scan rate from 20 to 500 mV s^{-1} within a voltage window of 3 V.

Please cite this article in press as: Z. Lin, et al., Journal of Power Sources (2016), http://dx.doi.org/10.1016/j.jpowsour.2016.04.035

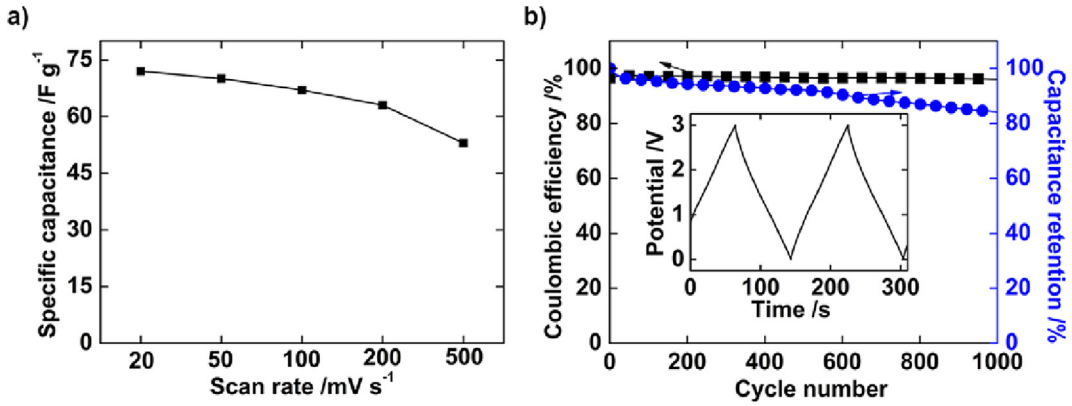

Fig. 4. a) Change of the specific capacitance with scan rate; b) Capacitance retention test of $Ti_3C_2T_x$ film at 1 A g^{-1} and coulombic efficiency of 2-electrode Swagelok cell.

the frequency is decreased, evidencing a slow ion dynamics in the electrode (Warburg region). Cyclic voltammograms (CVs) in a 2-electrode cell assembled with two identical electrodes are presented in Fig. 3b. The narrow CVs suggest an extremely low capacitance of less than 1 F g^{-1} at a scan rate of 20 mV s^{-1}.

Electrochemical performance of the $Ti_3C_2T_x$ ionogel films is presented in Fig. 3c and d. The Nyquist plot (Fig. 3c), shows a low high-frequency series resistance of 1.3 Ω cm^2; the resistance at the knee frequency is 20 Ω cm^2 corresponding to a resistance of the electrolyte in the MXene electrode of about 19 Ω cm^2 which is in the same range as that reported for graphene electrodes [22,23]. The fast increase of the imaginary part of the impedance at low frequency evidences a capacitive storage mechanism. Fig. 3d shows the CVs of a 2-electrode Swagelok cell assembled with two identical MXene electrodes, at scan rates from 20 mV s^{-1} to 500 mV s^{-1}. An average specific electrode capacitance of 70 F g^{-1} was obtained at a scan rate of 20 mV s^{-1} within a voltage window of 3 V. From our knowledge, this is the first report of MXene materials operating in an ionic liquid electrolyte with such a capacitance within a voltage window of 3 V. CVs of Fig. 3d show a set of peaks at about 0.5 V and 1.2 V. Differently from MXene in aqueous electrolytes, such features are not assumed to come from pseudocapacitive contributions of surface functional groups since O- or F- surface groups are not supposed to be electrochemically active in the aprotic ionic liquids [24]. The presence of these current peaks could be assigned to EMI^+ and/or $TFSI^-$ insertion between the $Ti_3C_2T_x$ layers such as those observed in layered MnO_2 [25,26] or for $Ti_3C_2T_x$ in organic electrolyte [17]; further in-situ XRD studies (in progress) will be needed to get a better insight of the capacitive charge storage mechanism. The capacitance change with the scan rate is shown in Fig. 4a; 75% of the capacitance is preserved when the scan rate is increased from 20 mV s^{-1} to 500 mV s^{-1}, which demonstrates the high power capability of the electrodes [27]. Fig. 4b shows the cell voltage variation with time during galvanostatic charge/discharge cycling tests (inset) as well as the related coulombic efficiency and capacitance retention (in %). As observed, after 1000 cycles, capacitance retention is still more than 80% of the initial capacitance while coulombic efficiency remains above 95%.

In addition, a thicker $Ti_3C_2T_x$ ionogel film (400 μm), with a mass loading of 4 mg cm^{-2} (mass of $Ti_3C_2T_x$ only) was investigated and found to perform similarly to the thin films. The Nyquist plot (Fig. 5a) shows the change of the imaginary vs. real part of the impedance. The high frequency series resistance is in the same range as that of thinner films (1.1 Ω cm^2). As expected, the ionic resistance of the $Ti_3C_2T_x$ electrode, calculated from the difference between the knee frequency resistance and the high frequency series resistance, was found to be slightly larger than that of the thinner film (22 Ω cm^2), which attributed to the larger thickness of the film [28]. A capacitive behavior can be observed from the CV plots in Fig. 5b. A capacitance of 70 F g^{-1} was achieved at a scan rate of 1 mV s^{-1} within a 3 V voltage window; the electrode was still delivering 90% (62 F g^{-1}) of the initial capacitance at 20 mV s^{-1}, thus showing decent power performance for this thick film in neat ionic liquid electrolyte.

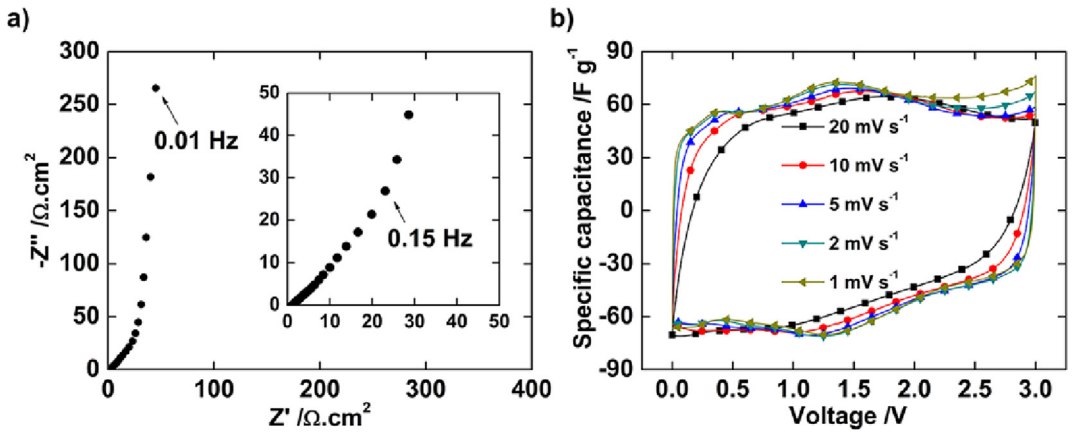

Fig. 5. Electrochemical characterization of thick $Ti_3C_2T_x$ ionogel film with mass loading of 4 mg cm^{-2} (mass of $Ti_3C_2T_x$ only): a) Nyquist plot of 2-electrode Swagelok cell; b) CVs of 2-electrode Swagelok cell with voltage window of 3 V.

Please cite this article in press as: Z. Lin, et al., Journal of Power Sources (2016), http://dx.doi.org/10.1016/j.jpowsour.2016.04.035

4. Conclusions

A $Ti_3C_2T_x$ MXene hydrogel was prepared by vacuum filtration. The hydrogel film was further immersed in EMI-TFSI ionic liquid electrolyte to prevent restacking of the MXene flakes after vacuum drying at 80 °C. Electrochemical performance of the $Ti_3C_2T_x$ ionogel film in EMI-TFSI ionic liquid electrolyte was compared to a vacuum-dried $Ti_3C_2T_x$ film. In contrast to the $Ti_3C_2T_x$ dried film exhibiting an extremely low capacitance of 1 F g^{-1} and a highly resistive behavior, the $Ti_3C_2T_x$ ionogel film shows a capacitance up to 70 F g^{-1} at a scan rate of 20 mV s^{-1} and a large voltage window of 3 V thanks to the disordered structure and larger $Ti_3C_2T_x$ interflake spacing. The capacitive signature is preserved at high scan rates (500 mV s^{-1}), suggesting high power performance as well. A thick $Ti_3C_2T_x$ ionogel film with high mass loading of 4 mg cm^{-2} shows a lower gravimetric capacitance of 62 F g^{-1} at a scan rate of 20 mV s^{-1}. To our knowledge, this is the first report on MXene hydrogel and also using MXene materials in an ionic liquid electrolyte, in which superior performance was achieved. Considering the rich chemistry of many other MXene materials, we can envisage further improvement by using MXenes in various ionic liquid electrolytes for supercapacitors.

Acknowledgements

Z. F. LIN was supported by China Scholarship Council (CSC). P. S. acknowledges the support from European Research Council (ERC, Advanced Grant, ERC-2011-AdG, Project no. 291543-IONACES). K. L. Van Aken and Y. Gogotsi were supported as part of the Fluid Interface Reactions, Structures and Transport (FIRST) Center, an Energy Frontier Research Center funded by the U.S. Department of Energy, Office of Science, Office of Basic Energy Sciences.

References

[1] M. Ghidiu, M.R. Lukatskaya, M.-Q. Zhao, Y. Gogotsi, M.W. Barsoum, Nature 516 (2014) 78–81.
[2] B. Anasori, Y. Xie, M. Beidaghi, J. Lu, B.C. Hosler, L. Hultman, P.R.C. Kent, Y. Gogotsi, M.W. Barsoum, ACS Nano 9 (2015) 9507–9516.
[3] M. Naguib, Y. Gogotsi, Accounts Chem. Res. 48 (2015) 128–135.
[4] M. Naguib, V.N. Mochalin, M.W. Barsoum, Y. Gogotsi, Adv. Mater. 26 (2014) 992–1005.
[5] M. Naguib, J. Come, B. Dyatkin, V. Presser, P.-L. Taberna, P. Simon, M.W. Barsoum, Y. Gogotsi, Electrochem. Commun. 16 (2012) 61–64.
[6] M. Naguib, J. Halim, J. Lu, K.M. Cook, L. Hultman, Y. Gogotsi, M.W. Barsoum, J. Am. Chem. Soc. 135 (2013) 15966–15969.
[7] O. Mashtalir, M.R. Lukatskaya, M.Q. Zhao, M.W. Barsoum, Y. Gogotsi, Adv. Mater. 27 (2015) 3501–3506.
[8] Z.Y. Lin, D.F. Sun, Q. Huang, J. Yang, M.W. Barsoum, X.B. Yan, J. Mater. Chem. A 3 (2015) 14096–14100.
[9] D.D. Sun, M.S. Wang, Z.Y. Li, G.X. Fan, L.Z. Fan, A.G. Zhou, Electrochem. Commun. 47 (2014) 80–83.
[10] D. Er, J. Li, M. Naguib, Y. Gogotsi, V.B. Shenoy, ACS Appl. Mater. Interfaces 6 (2014) 11173–11179.
[11] M.R. Lukatskaya, O. Mashtalir, C.E. Ren, Y. Dall'Agnese, P. Rozier, P.L. Taberna, M. Naguib, P. Simon, M.W. Barsoum, Y. Gogotsi, Science 341 (2013) 1502–1505.
[12] M. Hu, Z. Li, H. Zhang, T. Hu, C. Zhang, Z. Wu, X. Wang, Chem. Commun. 51 (2015) 13531–13533.
[13] X. Wang, S. Kajiyama, H. Iinuma, E. Hosono, S. Oro, I. Moriguchi, M. Okubo, A. Yamada, Nat. Commun. 6 (2015) 1–6.
[14] H.-W. Wang, M. Naguib, K. Page, D.J. Wesolowski, Y. Gogotsi, Chem. Mat. (2015) 349–359.
[15] M.-Q. Zhao, C.E. Ren, Z. Ling, M.R. Lukatskaya, C. Zhang, K.L. Van Aken, M.W. Barsoum, Y. Gogotsi, Adv. Mater. 27 (2015) 339–345.
[16] P. Yan, R. Zhang, J. Jia, C. Wu, A. Zhou, J. Xu, X. Zhang, J. Power Sources 284 (2015) 38–43.
[17] Y. Dall'Agnese, P. Rozier, P.-L. Taberna, Y. Gogotsi, P. Simon, J. Power Sources 306 (2016) 510–515.
[18] M. Armand, F. Endres, D.R. MacFarlane, H. Ohno, B. Scrosati, Nat. Mater. 8 (2009) 621–629.
[19] M.A. Hope, A.C. Forse, K.J. Griffith, M.R. Lukatskaya, M. Ghidiu, Y. Gogotsi, C.P. Grey, Phys. Chem. Chem. Phys. 18 (2016) 5099–5102.
[20] T.N. Blanton, D. Majumdar, Powder Diffr. 27 (2012) 104–107.
[21] M. Naguib, O. Mashtalir, J. Carle, V. Presser, J. Lu, L. Hultman, Y. Gogotsi, M.W. Barsoum, ACS Nano 6 (2012) 1322–1331.
[22] W.Y. Tsai, R.Y. Lin, S. Murali, L.L. Zhang, J.K. McDonough, R.S. Ruoff, P.L. Taberna, Y. Gogotsi, P. Simon, Nano Energy 2 (2013) 403–411.
[23] Z. Lin, P.-L. Taberna, P. Simon, Electrochim. Acta (2015), http://dx.doi.org/10.1016/j.electacta.2015.12.097 (in press).
[24] E. Kowsari, High-performance supercapacitors based on ionic liquids and a graphene nanostructure, in: S. Handy (Ed.), Ionic Liquids – Current State of the Art, InTech, 2015, pp. 505–542.
[25] J.-K. Chang, M.-T. Lee, W.-T. Tsai, M.-J. Deng, I.W. Sun, Chem. Mat. 21 (2009) 2688–2695.
[26] T.M. Benedetti, F.F.C. Bazito, E.A. Ponzio, R.M. Torresi, Langmuir 24 (2008) 3602–3610.
[27] D. Chunsheng, P. Ning, Nanotechnology 17 (2006) 5314.
[28] P.L. Taberna, P. Simon, J.F. Fauvarque, J. Electrochem. Soc. 150 (2003) A292–A300.